Comparison of Pilot-Assisted and Blind CDMA Array-Receivers Adaptive to Rayleigh Fading Rates*

Sofiène AFFES and Paul MERMELSTEIN
INRS-Télécommunications, Université du Québec
16, Place du Commerce, Ile-des-Soeurs, Verdun, H3E 1H6, Canada

Abstract— **Adaptive array-receivers for CDMA significantly increase performance and are expected to play a key role in future CDMA systems. In this contribution we compare the uplink performance of pilot-assisted and blind CDMA array-receivers adaptive to the Rayleigh fading conditions. We exploit these results to minimize identification errors and optimize capacity of array-receivers at different qualities of service and fading rates. Optimal pilot-to-data power ratios are suggested for pilot-assisted array-receivers. Evaluation results suggest power-ratios increasing with higher fading rates from 15 to 35%. Results also suggest that blind array-receivers perform better than pilot-assisted versions, especially at higher fading rates and smaller BER values. The advantage of blind array-receivers also increases with an increase in the number of antennas.**

I. Introduction

To increase the uplink capacity of wideband applications in wireless CDMA [1], future standards are expected to implement coherent detection with a pilot. This pilot should allow the identification of the channel and the estimation of its phase offset in particular. Many works previously analyzed the performance of pilot-assisted systems in Rayleigh fading channels [2]-[5]. Study of the effects of channel estimation errors on performance [3],[4],[6] is of particular interest in pilot-assisted schemes. It allows optimization of performance [2],[4],[5] and the allocation of an optimal pilot-to-data power ratio in particular [4],[5].

We extend previous works and consider the analysis and evaluation of pilot-assisted CDMA array-receivers adaptive to Rayleigh fading. We also include the case of blind array-receivers for comparative evaluation. Indeed, array-receivers for CDMA significantly increase performance [7] and are expected to play a key role in future CDMA systems. We first perform a performance and convergence analysis of channel identification by adaptive array-receivers and validate it by simulations. This analysis takes into account adaptation of array-receivers to the time-variations of the Rayleigh channel at different fading rates. It allows the selection of an optimal adaptation step-size for the minimization of identification errors at different operating conditions of noise and fading rate. These results lead to a simple method for capacity computation to evaluate and optimize pilot-assisted and blind adaptive array-receivers at different qualities of service and fading rates. Optimal pilot-to-data power ratios may be readily selected for pilot-assisted array-receivers. Evaluation results suggest that blind array-receivers perform better than pilot-assisted versions at higher fading rates and qualities of service.

* Work supported by the Bell Quebec/Nortel/NSERC Industrial Research Chair in Personal Communications.

II. Formulation and Background

We denote by M the number of the uplink receiving antennas at the base-station and consider a multipath Rayleigh fading environment with a number of paths P and a Doppler frequency f_D. The data is BPSK modulated at the rate $1/T_s$ where T_s is the symbol duration. After despreading, we obtain the post-correlation model (PCM) [8],[9] of the received signals over the $M \times P$ spatio-temporal diversity branches in the observation vector:

$$\underline{\mathrm{Z}}_n = \underline{\mathrm{H}}_n s_n + \underline{\mathrm{N}}_n = \underline{\mathrm{H}}_n \psi_n b_n + \underline{\mathrm{N}}_n \ , \qquad (1)$$

where $s_n = \psi_n b_n$ is the signal component, b_n is the BPSK data sequence and ψ_n^2 is the total received power. For sake of simplicity, we assume a perfect power control situation (*i.e.*, the total received power is $\psi_n^2 = \psi^2$) and relegate the case of imperfect power control to a future study. $\underline{\mathrm{H}}_n$ is the $M \times P$ spatio-temporal Rayleigh fading channel vector normalized to $\sqrt{M}$ (see [8],[9]). Finally, $\underline{\mathrm{N}}_n$ is a white Gaussian interference vector with mean zero and variance σ_N^2 after despreading. The resulting input SNR after despreading is $SNR_{\text{in}} = \psi^2/\sigma_N^2$ per antenna element.

For analysis and evaluation of adaptive array-receivers, we select the spatio-temporal array-receiver (STAR) [8] as a study-case for its simplicity and performance efficiency. This array-receiver is also representative of a wider class of array-receivers relying on principal component analysis [7]. In addition, it allows implementation of different combining and detection schemes.

STAR first performs simple signal component extraction by spatio-temporal maximum ratio-combining (MRC):

$$\hat{s}_n = \text{Real}\left\{ \frac{\hat{\underline{\mathrm{H}}}_n^H \underline{\mathrm{Z}}_n}{M} \right\} \ , \qquad (2)$$

then feeds this result back in a decision feedback identification (DFI) scheme to arrive at a blind channel

identification procedure (see details in [8]):

$$\underline{\hat{\mathrm{H}}}_{n+1} = \underline{\hat{\mathrm{H}}}_n + \mu \left(\underline{\mathrm{Z}}_n - \underline{\hat{\mathrm{H}}}_n \hat{s}_n \right) \hat{s}_n, \tag{3}$$

where $\underline{\hat{\mathrm{H}}}_n$ is the adaptive channel estimate and μ is the adaptation step-size.

The simple DFI scheme of Eqs. (2) and (3) allows coherent detection of the signal component within a sign ambiguity [8] and requires differential decoding of DBPSK modulated data. If we drop the real part in (2), we can simulate techniques that implement differential demodulation with a loss in capacity performance by almost a factor 2 [8]. However, such methods will not be pursued here. Optimum combining could be used instead of MRC to determine the feedback signal [13], but this version will not be analyzed here for the sake of simplicity. Finally, if a known reference signal s_n such as a pilot is used for feedback, we obtain a well known least mean square (LMS) gradient-type [11] tracking equation as the pilot-channel-assisted version of STAR.

Using classical LMS analysis techniques [11], we analyze next the performance and convergence of identification by STAR assuming for the sake of simplicity the use of a well known reference (*i.e.*, pilot-assisted version). Exact derivations for the blind version could be made, but we shall see that analysis results still hold in the case of decision feedback instead of a known reference. Later, we exploit these results to evaluate and optimize capacity for the pilot-assisted (*i.e.*, coherent detection) and the blind (*i.e.*, coherent detection and differential decoding) array-receivers.

III. Performance and Convergence Analyses

For the sake of clarity and brevity, we avoid mathematical derivations and directly provide the main performance and convergence analyses results. These results are validated by simulations to provide best choices of the step-size μ that achieves optimized channel identification and capacity at different operating conditions of noise and fading rate.

A. Theoretical Results

First, we show that the step-size μ should be bounded:

$$0 < \mu < \mu_{\max} \ , \tag{4}$$

where the maximum step-size $\mu_{\max}$ is given by:

$$\mu_{\max} = \frac{2}{\psi^2} \ . \tag{5}$$

This equation known as the *stability condition* guarantees convergence of the propagation channel estimator. If μ satisfies this condition, the propagation channel estimator $\underline{\hat{\mathrm{H}}}_n$ is locally biased at convergence by:

$$\bar{\Delta}\underline{\mathrm{H}}_n = -\tau_1 \dot{\underline{\mathrm{H}}}_n \ , \tag{6}$$

where the *time constant* to convergence in the mean sense τ_1 is given by:

$$\tau_1 = \frac{1}{\mu\psi^2} \ , \tag{7}$$

and where the channel speed vector $\dot{\underline{\mathrm{H}}}_n$ is locally approximated by:

$$\dot{\underline{\mathrm{H}}}_n = \frac{\underline{\mathrm{H}}_n - \underline{\mathrm{H}}_{n-\tau_1}}{\tau_1} \ . \tag{8}$$

The time constant τ_1 is the number of iterations required for convergence of the tracking procedure. It introduces a response delay to the channel time-variations and leads to a bias in channel estimation. On average, this local bias $\bar{\Delta}\underline{\mathrm{H}}_n$ is centered. However, its contribution in the mean square sense reflects the temporal correlation of Rayleigh fading and cannot be neglected, as shown next.

Indeed, we establish that the *steady-state misadjustment* at convergence is given by:

$$\begin{aligned} \beta^2(\mu, \sigma_N^2, f_D T_s) &= \frac{E\left[\|\Delta\underline{\mathrm{H}}_n\|^2\right]}{MP} = \frac{E\left[\|\underline{\hat{\mathrm{H}}}_n - \underline{\mathrm{H}}_n\|^2\right]}{MP} \\ &= \beta_N^2(\mu, \sigma_N^2) + \beta_D^2(\mu, f_D T_s) \ , \end{aligned} \tag{9}$$

where the *time constant* to convergence in the mean square sense τ_2 is given by:

$$\tau_2 = \frac{1}{2\mu\psi^2 \left(1 - \frac{\mu}{\mu_{\max}}\right)} \ . \tag{10}$$

Equation (9) shows that misadjustment is the sum of two terms. The first, $\beta_N^2(\mu, \sigma_N^2)$, is the contribution of errors due to noise and corresponds to the misadjustment when the channel is static (*i.e.*, $f_D = 0$ Hz):

$$\beta_N^2(\mu, \sigma_N^2) = \frac{\tau_2}{\tau_1} \mu \sigma_N^2 \ . \tag{11}$$

It increases with higher values of μ and lower SNR levels as adaptation perturbations around the optimal solution increase at steady-state. The second term, $\beta_D^2(\mu, f_D T_s)$, is the contribution of errors due to the tracking response delay to the channel time-variations. It represents the misadjustment if the received signal is noise-free (*i.e.*, $\sigma_N^2 = 0$):

$$\beta_D^2(\mu, f_D T_s) = \frac{2}{P} \left\{ 1 - \mathcal{B}_0 \left(2\pi f_D T_s \tau_1 \right) \right\} \ , \tag{12}$$

where $\mathcal{B}_0(x)$ is the Bessel function of the first kind of order 0. This term increases with smaller values of μ and higher fading rates $f_D T_s$ as the tracking response delay and the channel time-variations increase respectively.

As confirmed by the solid-line theoretical curves of Figs. 1a to 3a (see details next), there is a tradeoff between the contributions of the two mean-square identification error terms mentioned above, resulting in a

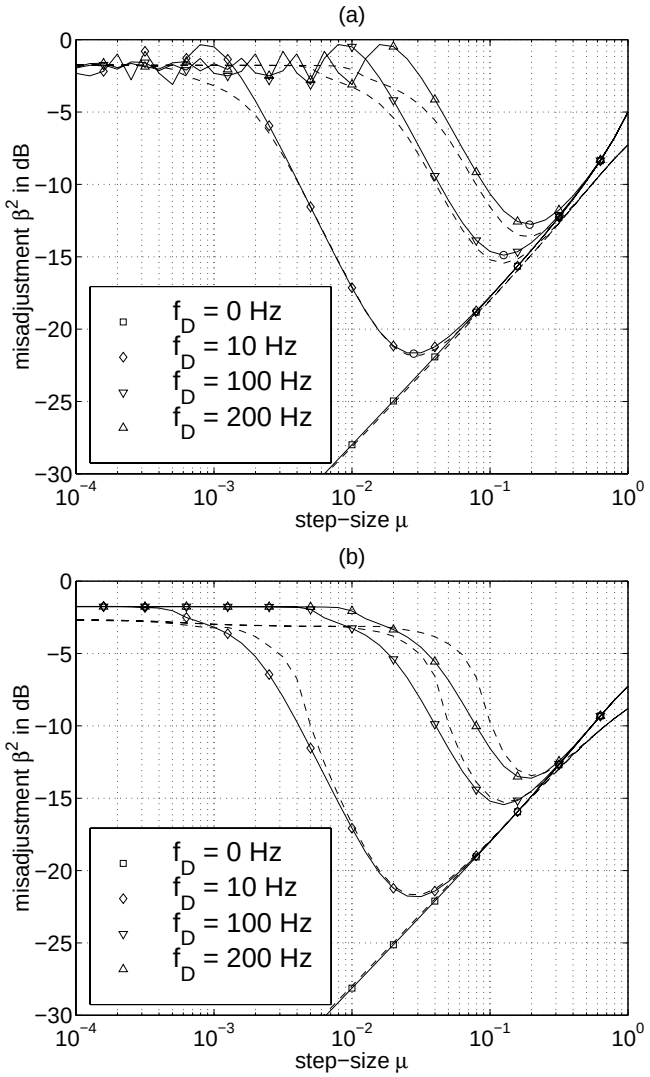

Fig. 1. Misadjustment β^2 vs. step-size μ for different values of f_D at $SNR_{\text{in}} = 5$ dB. (a): theoretical (solid), experimental with reference (dashed), optimal point ('o'). (b): experimental with reference (solid), experimental with feedback (dashed).

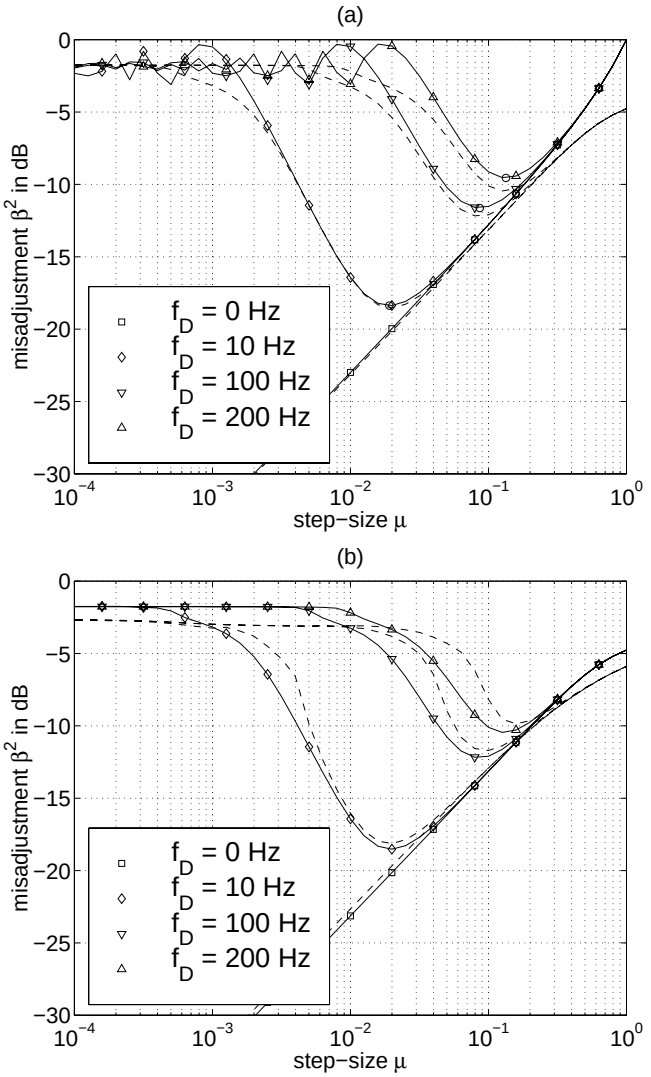

Fig. 2. Misadjustment β^2 vs. step-size μ for different values of f_D at $SNR_{\text{in}} = 0$ dB. (a): theoretical (solid), experimental with reference (dashed), optimal point ('o'). (b): experimental with reference (solid), experimental with feedback (dashed).

minimum misadjustment $\beta^2_{\min}$ achievable at an optimal step-size $\mu_{\text{opt}}^{\beta^2}$ (see points marked with 'o'). For lower values of μ, the channel identification procedure of Eq. (3) is less able to track time-variations and β_D^2 increases. For higher values, perturbations due to adaptation in (3) are higher and β_N^2 increases. In either case, the total misadjustment β^2 increases. In the following, we validate the above analysis results by simulations.

B. Validation and Discussion

To illustrate and validate the previous theoretical analysis results, we consider the case of $M = 4$ antennas and $P = 3$ equal power paths. Three Doppler frequency values of 10, 100 and 200 Hz are examined, corresponding to three representative mobile speeds of almost 5, 50 and 110 km/h respectively (*i.e.*, pedestrian, urban and highway) at a carrier frequency of 1.9 GHz. These Doppler frequencies correspond to fading rates of almost 5.2×10^{-4}, 5.2×10^{-3} and 10^{-2} respectively at a data baud rate of 19.2 kb/s. The static-channel case (*i.e.*, $f_D = 0$ Hz) is included as a reference. Independent Rayleigh fading is simulated using Jakes' model [12]. Experimental values of misadjustment are obtained by averaging the mean-square identification error over 100,000 symbol iterations after convergence.

In Fig. 1a, we show the theoretical and experimental misadjustment curves to validate the analysis results at a practical SNR value of 5 dB. A good fit is observed between the two curves, except for very small values of μ where the dominant misadjustment term is due to tracking delay of the Rayleigh fading channel. In that region, the theoretical curve displays sidelobes due to the temporal correlation of Rayleigh fading (*i.e.*, Bessel function). On the other hand, these

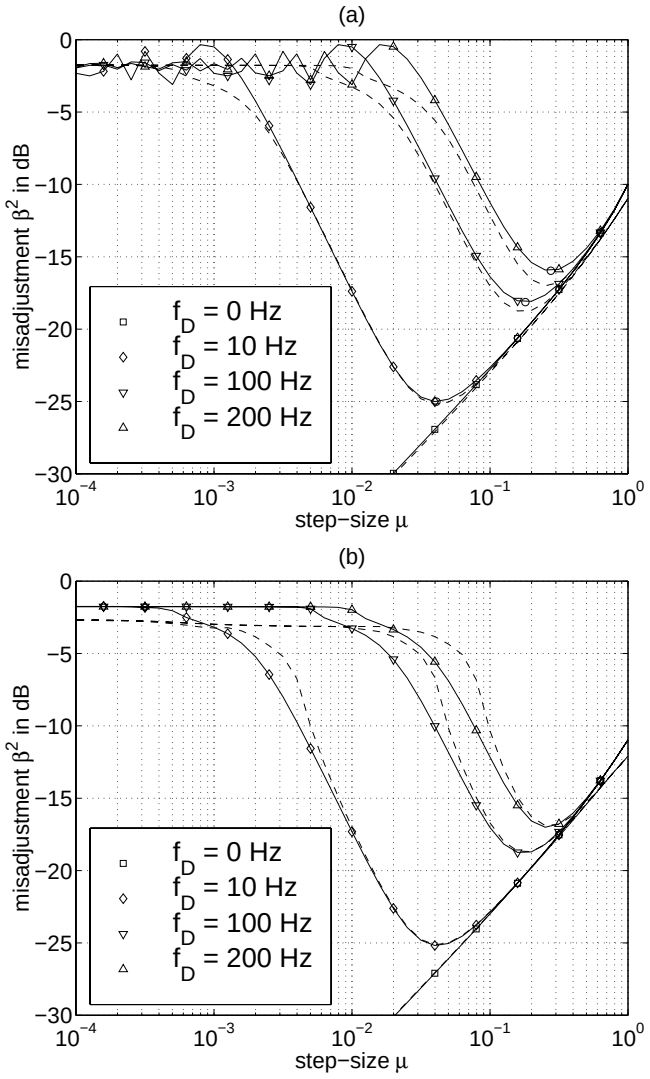

Fig. 3. Misadjustment β^2 vs. step-size μ for different values of f_D at $SNR_{\text{in}} = 10$ dB. (a): theoretical (solid), experimental with reference (dashed), optimal point ('o'). (b): experimental with reference (solid), experimental with feedback (dashed).

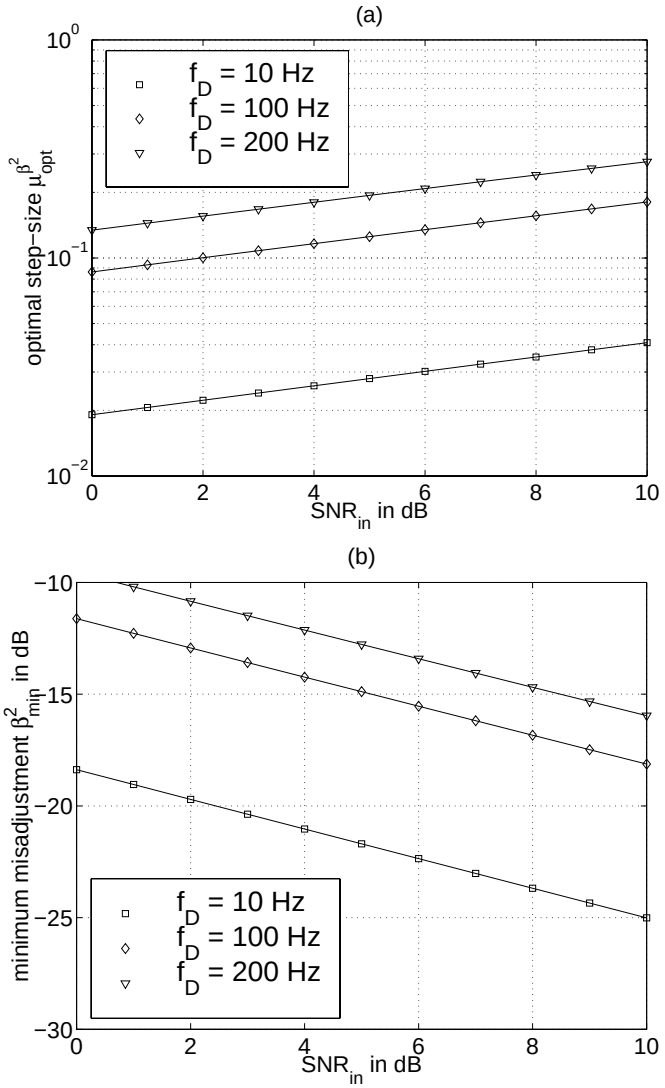

Fig. 4. (a): optimal step-size $\mu_{\text{opt}}^{\beta^2}$ vs. input SNR SNR_{in} for different values of f_D. (b): minimum misadjustment β_{min}^2 vs. input SNR SNR_{in} for different values of f_D.

sidelobes are not present in the experimental curve due to the inaccuracy of the temporal correlation profile of the Jakes' Rayleigh fading generator outside the main lobe of the Bessel function. In the absence of fading, the two curves coincide even for small values of μ.

In Fig. 1b, we compare the experimental misadjustment curve of Fig. 1a obtained with an exact reference (*i.e.*, analysis assumption) with the experimental curve obtained with feedback. We observe again that the two curves almost coincide, especially at smaller Doppler frequencies, and at values of μ around $\mu_{\text{opt}}^{\beta^2}$ where the minimum misadjustment β_{min}^2 is achieved. This figure shows that the theoretical analysis results obtained hold for either pilot-assisted or blind array-receivers. Figs. 2a and 3a replicate Fig. 1a at SNR values of 0 and 10 dB, respectively. They validate the theoretical analysis results over a wider SNR range. Figs. 2b and 3b indicate that the approximation of the blind array-receiver performance curves by the theoretical ones is better at higher SNR levels.

Figures 1 to 3 all suggest that the theoretical optimal step-size values provide very good approximations to achieve optimal performance in practice with either pilot-assisted or blind array-receivers at different operating conditions of noise or fading rate. In any case, the optimal step-size $\mu_{\text{opt}}^{\beta^2}$ is located in the main lobe of the Bessel function and is bounded by:

$$\frac{\pi}{2} f_D T_s < \mu_{\text{opt}}^{\beta^2} < \mu_{\max} \ . \tag{13}$$

Therefore, the optimum step-size shown in Fig. 4a can be obtained in practice by a simple search over μ that minimizes β^2 between these bounds. At specified operating conditions of noise and fading rate, resulting minimum misadjustment values are shown in Fig. 4b and given by:

$$\beta_{\text{min}}^2(\sigma_N^2, f_D T_s) = \beta^2(\mu_{\text{opt}}^{\beta^2}, \sigma_N^2, f_D T_s) \ . \tag{14}$$

Higher fading rates require higher values of $\mu_{\rm opt}^{\beta^2}$ (see Fig. 4a) and increase the minimum misadjustment (see Fig. 4b). Higher SNR levels also require higher values of $\mu_{\rm opt}^{\beta^2}$ (see Fig. 4a) to allow for better tracking of channel time-variations, but reduce the minimum misadjustment (see Fig. 4b). In the static-channel case not shown in Fig. 4, β^2 decreases monotonically to 0 with decreasing values of μ regardless of the SNR level, resulting in optimal step-size and misadjustment values both asymptotically equal to 0.

To specify operating conditions in practice, a Doppler frequency estimator (*e.g.*, [13]) can be used to estimate $\hat{f}_D$ while $\hat{\sigma}_N^2$ and $\hat{\psi}^2$ can be both estimated from the received signals. The estimated value $\hat{\mu}_{\rm opt}^{\beta^2}$ is derived from the minimization of $\beta^2(\mu) = \beta^2(\mu, \hat{\sigma}_N^2/\hat{\psi}^2, \hat{f}_D T_s)$ and incorporated in (3) to optimize channel identification and achieve $\beta_{\rm min}^2$. We next evaluate the impact of optimized channel identification on capacity for both pilot-assisted and blind array-receivers.

IV. Capacity Evaluation

Using the analysis results established earlier, we first propose simple computation procedures to evaluate and optimize the uplink capacity in terms of number of users per cell for both pilot-assisted and blind array-receivers at different qualities of service and fading rates (*i.e.*, operating conditions). Second, we provide and discuss optimized capacity evaluation results and compare the performance of pilot-assisted and blind array-receivers.

A. Computation Procedures

Capacity computation procedures for pilot-assisted and blind array-receivers, shown in Fig. 5, have the same general structure. For a specified bit-error rate (BER) value before channel decoding, say p_e (*i.e.*, quality of service), both procedures compute the bit energy to noise ratio $\frac{E_b}{N_o}$ required. After initialization, they increment the capacity, C, until the corresponding output SNR established by analysis and given by:

$$SNR_{\rm out} = SNR_{\rm in}\ \frac{2M}{1+(P+SNR_{\rm in})\beta^2}\ , \qquad (15)$$

no longer exceeds the required $\frac{E_b}{N_o}$. C is then reduced to the largest value for which $SNR_{\rm out} \geq \frac{E_b}{N_o}$. However, the two procedures differ in steps 1, 3.2 and 3.3 computing $\frac{E_b}{N_o}$, the noise variance σ_N^2 and misadjustment β^2 respectively.

In step 1, for pilot-assisted array-receivers we compute the $\frac{E_b}{N_o}$ required with coherent detection (see Fig. 5a). However, for blind array-receivers we compute the $\frac{E_b}{N_o}$ required with coherent detection and differential decoding (see Fig. 5b) assuming the worst case of

(a)

1. Find $\frac{E_b}{N_o} = \text{erfinv}(1-2p_e)^2$.
2. Initialize capacity $C = 0$.
3. Start computation loop:
  3.1. increment capacity $C = C + 1$,
  3.2. compute noise variance
    $\sigma_N^2 = \frac{C(1+\xi^2)(1+\eta^2)}{L}$,
  3.3. compute misadjustment
    $\beta^2(\mu, \sigma_N^2/\xi^2, f_D T_s)$,
  3.4. compute output SNR
    $SNR_{\rm out} = SNR_{\rm in}\ \frac{2M}{1+(P+SNR_{\rm in})\beta^2}$,
  3.5. if $SNR_{\rm out} \geq \frac{E_b}{N_o}$ goto **3.1**, else exit loop.
4. Decrement capacity $C = C - 1$.

(b)

1. Find $\frac{E_b}{N_o} = \text{erfinv}(1-p_e)^2$.
2. Initialize capacity $C = 0$.
3. Start computation loop:
  3.1. increment capacity $C = C + 1$,
  3.2. compute noise variance
    $\sigma_N^2 = \frac{C(1+\eta^2)}{L}$,
  3.3. compute misadjustment
    $\beta^2(\mu, \sigma_N^2, f_D T_s)$,
  3.4. compute output SNR
    $SNR_{\rm out} = SNR_{\rm in}\ \frac{2M}{1+(P+SNR_{\rm in})\beta^2}$,
  3.5. if $SNR_{\rm out} \geq \frac{E_b}{N_o}$ goto **3.1**, else exit loop.
4. Decrement capacity $C = C - 1$.

Fig. 5. Capacity computation procedures at a specified fading rate $f_D T_s$. (a): $C^p(p_e, \mu, \xi^2)$ for pilot-assisted array-receivers (*i.e.*, coherent detection). (b): $C^b(p_e, \mu)$ for blind array-receivers (*i.e.*, coherent detection and differential decoding).

error propagation in differential decoding (*i.e.*, multiplied by 2). This scenario should compensate for the fact that the theoretical misadjustment used in the case of blind array-receivers is over-optimistic, especially at higher BER values (*i.e.*, lower SNR levels).

In step 3.2, we use the fact that each in-cell user is received with a total received power of $(1+\xi^2)\psi^2$ for pilot-assisted and ψ^2 for blind array-receivers respectively, where ξ^2 denotes the pilot-to-data power ratio allocated for the pilot-assisted array-receiver. Hence the in-cell interference powers before despreading resulting from C in-cell users are $C(1+\xi^2)\psi^2$ and $C\psi^2$, respectively. Assuming that the outcell-to-incell interference ratio is η^2 [1], the total received interference powers before despreading are $C(1+\xi^2)(1+\eta^2)\psi^2$ and $C(1+\eta^2)\psi^2$ respectively. Steps 3.2 in Figs. 5a and 5b hence compute the received interference power

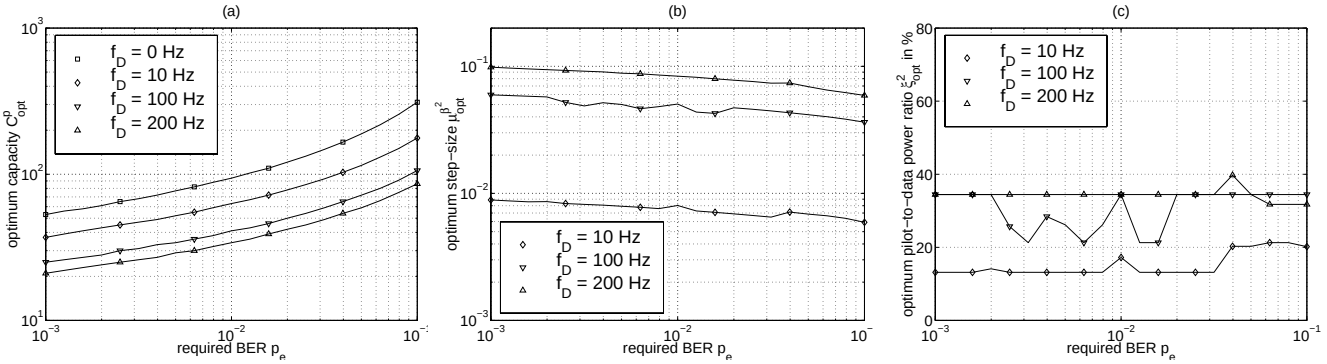

Fig. 6. Pilot-assisted array-receiver evaluation results versus the required BER p_e for different values of f_D. (a): optimum capacity C^p_{opt}. (b): optimum step-size $\mu^{\beta^2}_{\text{opt}}$. (c): optimum pilot-to-data power ratio ξ^2_{opt}.

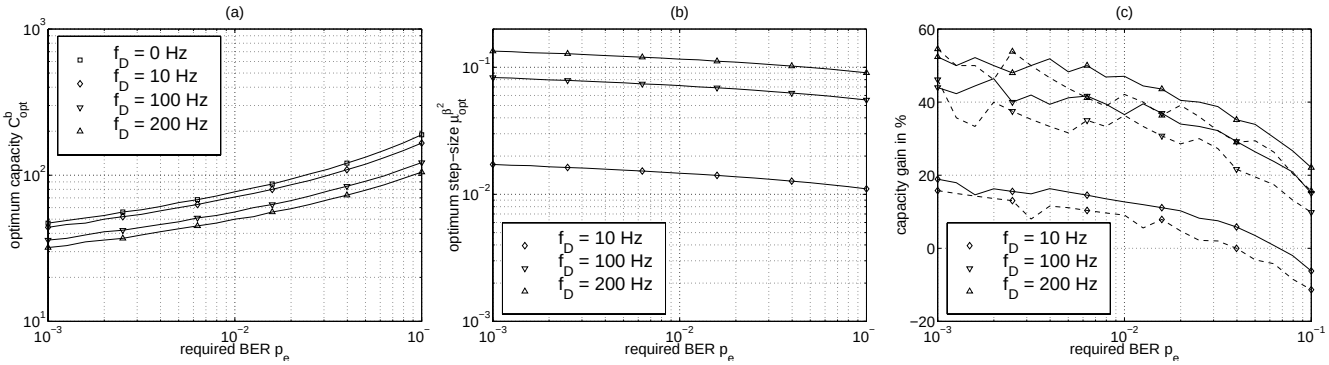

Fig. 7. Blind array-receiver evaluation results versus the required BER p_e for different values of f_D. (a): optimum capacity C^b_{opt}. (b): optimum step-size $\mu^{\beta^2}_{\text{opt}}$. (c): gain in capacity over pilot-assisted array-receiver (solid - $M = 4$, dashed - $M = 2$).

after despreading with a processing gain denoted by L assuming perfect power control (*i.e.*, $\psi^2 = 1$) for pilot-assisted and blind array-receivers respectively.

Finally in step 3.3, while misadjustment of identification with blind array-receivers in Fig. 5b is computed with a noise level of σ_N^2, misadjustment of identification with a pilot-assisted array-receiver is computed in Fig. 5a with a noise level of σ_N^2/ξ^2 seen form the pilot.

The two procedures of Fig. 5 provide simple capacity evaluation tools for pilot-assisted and blind array-receivers, but also allow optimization of capacity at different qualities of service and fading rates. At specified operating conditions, the optimal step-size $\mu^{\beta^2}_{\text{opt}}$ obtained in the previous section is used in step 3.3 to achieve the minimum misadjustment $\beta^2_{\min}$. Thus capacity expressions for blind and pilot-assisted array-receivers $C^b(p_e, \mu)$ and $C^p(p_e, \mu, \xi^2)$ are optimized over μ, resulting in $C^b_{\text{opt}}(p_e)$ and $C^p_{\text{opt}/\mu}(p_e, \xi^2)$ respectively.

We actually observed that $C^p_{\text{opt}/\mu}(p_e, \xi^2)$ always displays a unique maximum as a function of ξ^2. The tradeoff in ratio ξ^2 lies between a better reduction of identification errors from pilot with stronger values (see step 3.3, Fig. 5b) and a better reduction of received interference with weaker values (see step 3.3, Fig. 5b). Hence, similarly to the simple search over $\mu^{\beta^2}_{\text{opt}}$ described earlier below Eq. (13), $C^p_{\text{opt}/\mu}(p_e, \xi^2)$ is further optimized by a simple search over an optimal pilot-to-data power ratio ξ^2_{opt} that maximizes $C^p_{\text{opt}/\mu}(p_e, \xi^2)$, resulting in an optimal capacity for pilot-assisted array-receivers $C^p_{\text{opt}}(p_e) = C^p_{\text{opt}/\mu}(p_e, \xi^2_{\text{opt}})$.

B. Results and Discussion

We now compare optimal capacity results for pilot-assisted and blind array-receivers. We also give the corresponding optimal values of the step-size and the pilot-to-data power ratio at different qualities of service and fading rates. In addition to the parameters selected in subsection III-B, we consider for illustration the case of a processing gain $L = 64$ and an outcell-to-incell interference ratio $\eta^2 = 1$.

In Fig. 6, we provide evaluation results for the pilot-assisted array-receiver at different Doppler frequencies. In Fig. 6a, we show the optimal capacity in the static-channel case (*i.e.*, $f_D = 0$ Hz) for comparisons as an upper bound asymptotically reached with values of μ and ξ^2 both approaching 0. The pilot-assisted array-receivers suffer from a significant loss in capacity compared to the static-channel case. The results suggest that capacity is very sensitive to Rayleigh fading. It degrades rapidly at low Doppler frequencies, but more slowly as the Doppler frequency increases further.

Fig. 6b shows that the step-size selected for opti-

mization of capacity is almost constant over a wide range of qualities of service. Curves indicate values around 7×10^{-3}, 5×10^{-2} and 8×10^{-2} respectively to the Doppler frequencies selected. Similarly, Fig. 6c shows that the optimal pilot-to-data power ratio required for optimization of capacity varies a little over a wide range of BER values. As would be expected intuitively, the pilot-to-data power ratio increases from 15 to 35% with higher fading rates and covers the range of values suggested for practical systems.

In Fig. 7, we provide evaluation results for the blind array-receiver at different Doppler frequencies. Due to differential decoding, Fig. 7a shows that the upper bound curve of capacity asymptotically achievable in the static-channel case (*i.e.*, $f_D = 0$ Hz) is lower as compared to the same curve of Fig. 6a. Evidently blind array-receivers suffer from a relatively less significant loss in capacity. Their performance appears more robust to Rayleigh fading and results overall in a higher capacity as will be discussed below.

Similarly to Fig. 6b, Fig. 7b indicates that almost constant values of the optimal step-size can be selected for a wide range of BER values around 10^{-2}, 7×10^{-2} and 10^{-1} respectively to the Doppler frequencies considered.

Most importantly, we plot in Fig. 7c the gain in capacity of blind array-receivers over pilot-assisted array-receivers, given by $C^b(p_e)/C^p(p_e) - 1$. This figure suggests that blind array-receivers outperform pilot-assisted versions in almost all the situations studied, except for the case of large BER values required at low fading rates. It also suggests that the gain in capacity with blind array-receivers is more significant at higher fading rates and smaller BER values. At a practical value of $p_e = 6 \times 10^{-2}$ for the required BER before FEC decoding, Fig. 6c shows that pilot-assisted and blind array receivers almost achieve the same capacity at 10 Hz. On the other hand at Doppler frequencies between 100 and 200 Hz, a gain in capacity with blind array-receivers of 25 to 30 % is noted.

Finally we repeated the simulations with $M = 2$ antennas. For both array-receiver versions, capacity is almost reduced by half at all tested BER values and Doppler frequencies and the optimum step-size values remain almost constant. In the pilot-assisted version, the required pilot-to-data power ratio decreases by a negligible amount, showing that operating at higher interference levels with more antennas requires stronger pilots. Fig. 7c shows the gain in capacity of blind array-receivers over pilot-assisted array-receivers for $M = 2$ and 4 antennas. The curves indicate that the advantage of the blind array-receivers over the pilot-assisted ones increases with a larger number of antennas.

V. Conclusions

This work provides performance and convergence analyses of channel identification by pilot-assisted and blind CDMA array-receivers adaptive to Rayleigh fading validated by simulations. Our analysis allows the selection of an optimal adaptation step-size for the minimization of identification errors at different operating conditions of noise and fading rate. These results can be applied to derive a simple capacity computation tool that allows evaluation and optimization of pilot-assisted and blind adaptive array-receivers at different qualities of service and fading rates. For pilot-assisted array-receivers, this tool enables us to select an optimal pilot-to-data power ratio. Evaluation results suggest power-ratios increasing with higher fading rates from 15 to 35%, in the range of values suggested in practice. Our results suggest that blind array-receivers perform better than pilot-assisted versions at higher fading rates and smaller BER values, the difference increasing with more antennas, but are comparable at fading rates corresponding to portable terminals.

References

[1] A.J. Viterbi, *CDMA Principles of Spread Spectrum Communication*, Addison-Wesley, 1995.

[2] J.K. Cavers, "An analysis of pilot symbol assisted modulation for Rayleigh fading channels", *IEEE Transactions on Vehicular Technology*, vol. 40, no. 4, pp. 686-693, November 1991.

[3] F. Ling, "Coherent detection with reference-symbol based channel estimation for direct sequence CDMA uplink communications", *Proc. of IEEE VTC'93*, 1993, pp. 400-403.

[4] F. Ling, "Pilot assisted coherent DS-CDMA reverse-link communications with optimal robust channel estimation", *Proc. of IEEE ICASSP'97*, 1997, vol. 1, pp. 263-266.

[5] P. Schramm, "Analysis and optimization of pilot-channel-assisted BPSK for DS-CDMA systems", *IEEE Transactions on Communications*, vol. 46, no. 9, pp. 1122-1124, September 1998.

[6] X. Tang, M.-S. Alouini, and A. Goldsmith, "Effect of channel estimation error on M-QAM BER performance in Rayleigh fading", *Proc. of IEEE VTC'99*, 1999, vol. 2, pp. 1111-1115 (to appear also in *IEEE Transactions on Communications*).

[7] J. Thompson, P.M. Grant, and B. Mulgrew, "Performance of antenna array receiver algorithms for CDMA", *Signal Processing*, vol. 68, no. 1, pp. 23-41, July 1998.

[8] S. Affes and P. Mermelstein, "A new receiver structure for asynchronous CDMA : STAR - the spatio-temporal array-receiver", *IEEE Journal on Selected Areas in Communications*, vol. 16, no. 8, pp. 1411-1422, October 1998.

[9] W. Li, S. Affes, and P. Mermelstein, "Performance analysis of STAR for cellular CDMA systems", *Proc. of 19th Biennial Symposium on Communications*, Queen's University, 1998, pp. 271-275.

[10] H. Hansen, S. Affes, and P. Mermelstein, "A beamformer for CDMA with enhanced near-far resistance", *Proc. of IEEE ICC'99*, Vancouver, Canada, to appear, June 6-10, 1999.

[11] S. Haykin, *Adaptive Filter Theory*, Prentice-Hall, 1991.

[12] W.C. Jakes, Ed., *Microwave Mobile Communications*, John Wiley & Sons, 1974.

[13] H. Hansen, S. Affes, and P. Mermelstein, "A Rayleigh Doppler frequency estimator derived from ML theory", *Proc. of IEEE Signal Processing Workshop on Signal Processing Advances in Wireless Communications SPAWC'99*, 1999, pp. 382-386.